Steric Control of Reactivity of Non-Heme μ-Hydroxo Diiron(II) Complexes with Oxygen: Isolation of a Strongly Coupled μ-Oxo Fe(II)Fe(III) Dimer

Sonha C. Payne and Karl S. Hagen*

Contribution from the Department of Chemistry, Emory University, Atlanta, Georgia 30322

Received June 7, 1999. Revised Manuscript Received April 25, 2000

Abstract: The reactions of $[Fe_2(OH)(R_3CCOO)_2(Me_3tacn)_2]^+$ (R = F (**1**-F), Me (**1**-Me), Ph (**1**-Ph)) with dioxygen initially afford a μ-oxo bridged mixed valent diiron(II)(III) complex $[Fe_2O(R_3CCOO)_2(Me_3tacn)_2]^+$ (R = Me (**2**-Me) and Ph (**2**−Ph)) and subsequently the diiron(III) complexes **3**-Me and **3**-Ph. The reactions in acetonitrile are fast for **1**-F, slower for **1**-Me, and slow enough for **1**-Ph so that crystals of **2**-Ph as the triflate (**2**-Ph-OTf) and BPh_4 salts could be isolated and their structures determined. The oxidant *N*-methylmorpholine *N*-oxide (MMNO), is cleaner in that the byproduct, H_2O, does not further oxidize **2** as does the byproduct, H_2O_2, from the reaction with O_2. The crystal structures indicate that **2** has an oxo bridge with the Fe···Fe distances in **2**-Ph-OTf (3.123(1) Å) and **2**-Ph-BPh_4 (3.155(1) Å) similar to those of **3**. The magnetic susceptibility data are fit for **1**-Ph to two equivalent high-spin Fe(II) sites with $H = -2JS_1 \cdot S_2$, $D = 2.823$, $g = 2.00$, and $J = -12.1$ cm^{-1}, for **2**-Ph to an $S = {}^1/_2$ ground state with a high-spin Fe(III) site with $D = 1.46$, $g = 2.00$, and a high-spin Fe(II) site with $D = 13.93$, $E/D = 0.285$, $g = 2.069$, and $J = -144$ cm^{-1}, and for **2**-Me to an $S = {}^1/_2$ ground state with a high-spin Fe(III) site with $D = 2.39$, $g = 2.00$, and a high-spin Fe(II) site with $D = -11.42$, $g = 2.041$ and $J = -119$ cm^{-1}. The EPR spectrum is consistent with the $S = {}^1/_2$ ground state ($g = 1.97, 1.93, 1.90$ at 10 K) and is observed even at 85 K. The Mössbauer of **2**-Ph exhibits a poorly resolved doublet suggesting a Class II mixed valent species (Fe(II) and Fe(III) sites with $\delta = 1.09, 0.6$, $\Delta E_Q = 2.45, 2.35$, and $\Gamma = 0.55, 0.75$ mm s^{-1}, respectively). Electrospray mass spectra in MeCN with ^{18}O labeled **1**-−Ph and **1**-Me indicated that they reacted by an outer-sphere process with $^{16}O_2$ or MMN^{16}O as none of the oxidant is incorporated into **2**.

Introduction

The interaction of dioxygen with the diiron(II) complexes in non-heme proteins varies dramatically depending on the protein environment. Dioxygen reacts reversibly with hemerythrin (Hr), but is activated sufficiently by the diiron(II) sites in ribonucleotide reductase R2 (RNR-R2) and methane monooxygenase hydroxylase protein (MMOH) to generate a tyrosyl radical and to hydroxylate alkanes, respectively.[1−6] The iron storage protein, ferritin, also contains a metastable non-heme diiron site within a four-helix bundle that is believed to be a catalytic ferroxidase site for the oxidation of iron(II) prior to its storage within the protein.[7,8] The reversible binding of dioxygen to Hr involves a two-electron transfer in addition to a proton transfer to form a hydroperoxide bound diiron(III) μ-oxo-bridged site in which a hydrogen bond connects the hydroperoxide to the bridging oxide. A number of oxidation states and bridge configurations can exist during the reaction with dioxygen[9] prior to generation of the μ-oxo or μ-hydroxo diiron(III) species (met state). Among the more readily observed electronic confugurations are the $S = {}^1/_2$, mixed valent Fe(II)Fe(III) forms (e.g., semimet Hr) because of their relative stability and characteristic EPR signals with g_{av} less than 2.0. Early attempts to isolate synthetic models of mixed valent forms of these sites were unsuccessful[10] until multidentate, binucleating ligands were utilized.[11]

As part of our investigation of synthetic analogues of these proteins we have synthesized a number of carboxylate-bridged diiron(II) complexes and studied their reactivity in solution. To define the conditions under which these high-spin iron(II) complexes are formed, we have undertaken a study of the interaction of iron(II) salts with a variety of aliphatic or aromatic amines and carboxylates.[12] Dinuclear complexes bridged by carboxylates alone[12a,c] or two carboxylates and water were

(1) Waller, B. J.; Lipscomb, J. D. *Chem. Rev.* **1996**, *96*, 2625−2657.
(2) Nordlund, P.; Sjöberg, B.-M.; Eklund, H. *Nature* **1990**, *345*, 593−598.
(3) Nordlund, P.; Eklund, H. *J. Mol. Biol.* **1993**, *232*, 123−164.
(4) Logan, D. T.; Su, X.-D.; Åberg, A.; Regnström, K.; Hajdu, J.; Ecklund, H.; Nordlund, P. *Structure* **1996**, *4*, 1053−1064.
(5) Fox, B. D.; Surerus, K. K.; Münck, E.; Lipscomb, J. D. *J. Biol. Chem.* **1988**, *263*, 10553−10556.
(6) Rosenzweig, A. C.; Frederick, C. A.; Lippard, S. J.; Nordlund, P. *Nature* **1993**, *366*, 537−543. (b) Rosenzweig, A. C.; Nordlund, P.; Takahara, P. M.; Frederick, C. A.; Lippard, S. J. *Chem. Biol.* **1995**, *2*, 409−418.
(7) Harrison, P. M.; Arosio, P. *Biochim. Biophys. Acta* **1996**, *1275*, 161−203.
(8) Proulx-Curry, P. M.; Chasteen, N. D. *Coord. Chem. Rev.* **1995**, *144*, 347−368.
(9) Edmondson, D. E.; Huynh, B. H. *Inorg. Chim. Acta* **1996**, *252*, 399−404. (b) Kurtz, D. M., Jr. *J. Bio. Inorg. Chem.* **1997**, *2*, 159−167.
(10) Armstrong, W. H.; Spool, A.; Papaefthymiou, G. C.; Frankel, R. B.; Lippard, S. J. *J. Am. Chem. Soc.* **1984**, *106*, 3653−3667.
(11) Borovik, A. S.; Murch, B. P.; Que, L., Jr. *J. Am. Chem. Soc.* **1987**, *109*, 7190−7191. (b) Borovik, A. S.; Que, L., Jr. *J. Am. Chem. Soc.* **1988**, *110*, 2345−2347. (c) Borovik, A. S.; Papaefthymiou, V.; Taylor, L. F.; Anderson, O. P.; Que, L. J. *J. Am. Chem. Soc.* **1989**, *111*, 6183−6195.
(12) Lachicotte, R. J. Ph.D. Thesis, Emory University, 1995. (b) Nair, V. S. Ph.D. Thesis, Emory University, 1996. (c) Randall, C. R.; Shu, L. J.; Chiou, Y. M.; Hagen, K. S.; Ito, M.; Kitajima, N.; Lachicotte, R. J.; Zang, Y.; Que, L., Jr. *Inorg. Chem.* **1995**, *34*, 1036−1039.

10.1021/ja991885l CCC: $19.00
Published on Web 06/23/2000

isolated.[13] We have found that the reactivity of water-bridged iron(II) model complexes can be altered dramatically by varying the size of the carboxylates[14,15] and the nature of the solvent.[13] NMR studies of metal or carboxylate exchange reactions indicate that the hydroxide dicarboxylate-bridged complexes, $[Fe^{II}_2(OH)(R_3CCOO)_2(Me_3tacn)_2]^+$ (R = H (**1**-H)[16] F (**1**-F)[17] Me (**1**-Me)),[18] are kinetically stable to exchange reactions of the metals or carboxylates in aprotic solvents on the time scale of NMR experiments.[19] Reactions of these and other diiron(II) complexes with dioxygen have frequently yielded transient green solutions before finally yielding di- or polynuclear μ-oxo iron(III) aggregates.[16c] Here we report the reactivity with dioxygen of modifications of **1**, namely **1**-Me and **1**-Ph, to afford initially a μ-oxo-bridged mixed valent diiron(II)(III) complex, $[Fe_2(O)(R_3CCOO)_2(Me_3tacn)_2]^+$ (R = Me (**2**-Me) and Ph (**2**-Ph)). The acetate analogue, **2**-H, has been generated in solution and partially characterized.[16b,c] A preliminary report of part of this work has previously been reported. [20]

Experimental Section

Synthetic Methods. Triflic acid was used as obtained from 3M Co. $Fe(OTf)_2\cdot 2MeCN$ was prepared in a manner analogous to the Mn salt,[21] by reacting Fe metal and triflic acid in acetonitrile and crystallizing the product by adding ether. 1,4,7-Trimethyl-1,4,7-triazacyclononane (Me_3tacn) was prepared as previously described[22] and $(CD_3)_3$tacn was prepared in a similar manner using CD_2O and DCOOD in D_2O. The syntheses of this ligand and $(CD_2H)_3$tacn by a similar method have recently been reported.[23] *N*-Methylmorpholine *N*-oxide (MMNO) was obtained from Aldrich and recrystallized from acetone. Freshly prepared Dabco$(H_2O_2)_2$ was isolated from 50% H_2O_2 and Dabco in diethyl ether.[24] Elemental analyses were performed by Atlantic Microlabs, Inc. Atlanta, GA.

$[Fe^{II}_2(OH)(Ph_3CCO_2)_2(Me_3tacn)_2](OTf)$, 1-Ph-OTf: Neat Me_3tacn (0.342 g, 2.00 mmol) was added to a colorless solution of $Fe(OTf)_2\cdot 2CH_3CN$ (0.872 g, 2.00 mmol) in 5 mL of acetonitrile to give a dark purple solution. In a separate vial, triethylamine (417 uL, 3.00 mmol) was added to a slurry of triphenylacetic acid (0.576 g, 2.00 mmol) in 10 mL of acetonitrile to give a colorless solution, which when added to the purple solution caused it to turn yellow. Water (18 uL, 1.00 mmol) was added to the reaction mixture. After 24 h, off-white crystals of **1**-Ph (1.045 g, 87%) were collected by vacuum filtration, washed with cold acetonitrile followed by diethyl ether, and dried in vacuo. Crystals suitable for study by X-ray diffraction were obtained by recrystallization from acetonitrile. Anal. Calcd for $C_{59}H_{73}F_3Fe_2N_6O_8S$: C, 59.30; H, 6.16; N, 7.03. Found: C, 59.2; H, 6.1; N, 7.1.

$[Fe^{II}_2(OH)(Ph_3CCO_2)_2(Me_3tacn)_2](BPh_4)$, 1-Ph-BPh$_4$: A solution of **1**Ph-OTf (0.913 g, 0.764 mmol) in 40 mL of acetonitrile was treated with an excess of $NaBPh_4$ and allowed to stand at −20 °C whereupon 1.23 g (88% yield) of **1**-Ph-BPh_4 was isolated. Anal. Calcd for **1**-Ph-$BPh_4\cdot$MeCN, $C_{84}H_{96}BFe_2N_7O_5$: C, 71.75; H, 6.88; N, 6.97. Found: C, 71.4; H, 6.8; N, 7.1.

$[Fe^{II,III}_2O(Ph_3CCO_2)_2(Me_3tacn)_2](OTf)$, 2-Ph-OTf: Method 1. Off-white crystals of **1**-Ph (0.287 g, 0.24 mmol) were dissolved in 5 mL of acetonitrile to give a colorless solution. Dry dioxygen was bubbled through the solution for 5 min, resulting in a change in solution color from colorless through yellow to dark green. Reduction of the solvent volume in vacuo to 2 mL resulted in formation of dark green needles (0.096 g) of **2**-Ph that were collected by vacuum filtration, washed with cold acetonitrile followed by diethyl ether, and dried in vacuo. Diffusion of diethyl ether into the remaining dark green filtrate resulted in formation of additional dark green crystalline product (0.101 g, 67% total yield) that was collected by vacuum filtration, washed with cold acetonitrile and diethyl ether, and dried in vacuo. The less soluble **3**-Ph, which may be present due to slight over oxidation, may be removed by dissolving the dark green product in a minimal amount of acetonitrile and filtering the solution through a cotton plug.

Method 2. Dabco$\cdot H_2O_2$ (10.0 mL of a 2 mM acetonitrile solution, 0.20 mmol) was added to a colorless solution of **1**-Ph (0.478 g, 0.40 mmol) in 5 mL of acetonitrile. The reaction mixture was stirred at room temperature for 15 min during which time the solution color changed from colorless to dark green accompanied by formation of a white, microcrystalline precipitate. The white precipitate (68 mg) was removed by filtration and the volume of the dark green filtrate was reduced in vacuo to 5 mL. Addition of diethyl ether resulted in formation of **2**-Ph as dark green microcrystals (0.286 g, 60%) that were collected by vacuum filtration, washed with cold acetonitrile followed by diethyl ether, and dried in vacuo. The product was recrystallized by cooling a very concentrated acetonitrile solution to −30 °C, or by addition of diethyl ether to a cold, concentrated acetonitrile solution to afford dark green needles. Anal. Calcd for $C_{59}H_{72}F_3Fe_2N_6O_8S$: C, 59.35; H, 6.08; N, 7.04. Found: C, 58.8; H, 6.2; N, 7.1.

$[Fe^{II,III}_2O((Ph_3CCO_2)_2(Me_3tacn)_2](BPh_4)$, 2-Ph-BPh$_4$: Method 1. A pink solution of $NaBPh_4$ (0.691 g, 1.00 mmol) in 5 mL of acetonitrile was added to a dark green solution of **2**-Ph-OTf (0.597 g, 0.50 mmol) in 15 mL of acetonitrile. The solution was allowed to sit undisturbed at room temperature for 1 h during which time the formation of dark green crystals was observed. After one additional hour at −20 °C, the dark green needle crystals (0.574 g, 83%) were isolated by vacuum filtration, washed with 3 × 0.5 mL of cold acetonitrile followed by 1 mL of diethyl ether, and dried in vacuo. Recrystallization from acetonitrile/diethyl ether resulted in diffraction quality single crystals. Anal. Calcd for **2**-Ph-$BPh_4\cdot$MeCN, $C_{84}H_{95}BFe_2N_7O_5$: C, 71.80; H, 6.81; N, 6.98. Found: C, 71.7; H, 6.9; N, 7.1.

Method 2. Dry dioxygen was bubbled through a colorless solution of **1**-Ph-BPh_4 (0.704 g, 0.50 mmol) in 200 mL of acetonitrile for 1 h to give a dark green solution. Reduction of solvent volume in vacuo to 50 mL resulted in the formation of product as dark green needles (0.304 g, 44%) which were isolated by vacuum filtration, washed with diethyl ether, and dried in vacuo. Addition of excess solid $NaBPh_4$ to the orangish-red filtrate resulted in the formation of **3**-Ph-BPh_4, which was isolated from the filtrate as an orange powder (0.400 g, 24%).

Method 3. An amber solution of *N*-methylmorpholine *N*-oxide (0.059 g, 0.50 mmol) in 5 mL of acetonitrile was added to a colorless solution of 1-Ph-OTf (1.20 g, 1.00 mmol) in 200 mL of acetonitrile to give a dark green solution. Reduction of solvent volume in vacuo to 50 mL resulted in the formation of product as dark green needles (1.05 g, 91%) which were collected by vacuum filtration, washed with diethyl ether, and dried in vacuo.

$[Fe^{III}_2O(Ph_3CCO_2)_2(Me_3tacn)_2](OTf)_2$, 3-Ph-OTf: A colorless solution of sodium triflate (0.234 g, 2.00 mmol) in 3 mL of acetonitrile was added to a colorless solution of **1**-Ph-OTf (1.195 g, 1.00 mmol) in 15 mL of acetonitrile to give a pale yellow solution. Addition of an amber solution of MMNO (0.344 g, 2.00 mmol) in 2 mL of acetonitrile resulted in a change in solution color from pale yellow through green

(13) Hagen, K. S.; Lachicotte, R. J. *J. Am. Chem. Soc.* **1992**, *114*, 8741−8742.
(14) Hagen, K. S.; Lachicotte, R.; Kitaygorodskiy, A. *J. Am. Chem. Soc.* **1993**, *115*, 12617−12618.
(15) Hagen, K. S.; Lachicotte, R.; Kitaygorodskiy, A.; Elbouadili, A. *Angew. Chem., Int. Ed. Engl.* **1993**, *32*, 1321−1324.
(16) Chaudhuri, P.; Wieghardt, K.; Nuber, B.; Weiss, J. *Angew. Chem., Int. Ed. Engl.* **1985**, *24*, 778−779. (b) Hartman, J. R.; Rardin, R. L.; Chaudhuri, P.; Pohl, K.; Wieghardt, K.; Nuber, B.; Weiss, J.; Papaefthymiou, G. C.; Frankel, R. B.; Lippard, S. J. *J. Am. Chem. Soc.* **1987**, *109*, 7387−7396. (c) Feig, A. L.; Masschelein, A.; Bakac, A.; Lippard, S. J. *J. Am. Chem. Soc.* **1997**, *119*, 334−342.
(17) Lachicotte, R.; Kitaygorodskiy, A.; Hagen, K. S. *J. Am. Chem. Soc.* **1993**, *115*, 8883−8884.
(18) Abbreviations used: tacn, 1,4,7-triazacyclononane; Me_3tacn, 1,4,7-trimethyl-1,4,7-triazacyclononane; Tp, tri-1-pyrazolylborate.
(19) Hagen, K. S.; Kitaygorodskiy, A.; Blakesley, D. In preparation.
(20) Cohen, J. D.; Payne, S. C.; Hagen, K. S.; Sanders-Loehr, J. *J. Am. Chem. Soc.* **1997**, *119*, 2960−2961.
(21) Bryan, P. S.; Dabrowiak, J. C. *Inorg. Chem.* **1975**, *14*, 296−299.
(22) Wieghardt, K.; Chaudhuri, P.; Nuber, B.; Weiss, J. *Inorg. Chem.* **1982**, *21*, 3086−3090.
(23) Hage, R.; Gunnewegh, E. A.; Niel, J.; Tjan, F. S. B.; Weyhermuller, T.; Wieghardt, K. *Inorg. Chim. Acta* **1998**, *268*, 43−48.
(24) Oswald, A. A.; Guertin, D. L. *J. Org. Chem.* **1963**, *28*, 651−657.

to orange-red. Addition of diethyl ether followed by cooling the reaction mixture to −20 °C resulted in formation of **3**-Ph as orange-red plates which were collected by vacuum filtration, washed with diethyl ether, and dried in vacuo (1.230 g, 92%). Anal. Calcd for $C_{60}H_{72}F_6Fe_2N_6O_{11}S_2$: C, 53.66; H, 5.40; N, 6.26. Found: C, 53.5; H, 5.7; N, 6.2.

[$Fe^{III}_2O(Ph_3CCO_2)_2(Me_3tacn)_2$](BPh$_4$)$_2$, 3-Ph-BPh$_4$: A pink solution of sodium tetraphenylborate (0.208 g, 1.21 mmol) in 5 mL of acetonitrile was added to a colorless solution of **1**-Ph-BPh$_4$ (0.851 g, 0.610 mmol) in 100 mL of acetonitrile to give a pale yellow solution. Addition of an amber solution of MMNO (0.142 g, 1.21 mmol) in 5 mL of acetonitrile resulted in a change in solution color from pale yellow through green to reddish-orange. Reduction of the solvent volume in vacuo to 10 mL resulted in the formation of product as dark reddish-orange needles (0.730 g, 72%), which were collected by vacuum filtration, washed with diethyl ether, and dried in vacuo. The product was recrystallized by diffusing Et_2O into a DMF solution. Anal. Calcd for **3**-Ph-BPh$_4$·2DMF, $C_{112}H_{126}B_2Fe_2N_8O_7$: C, 73.53; H, 6.94; N, 6.12. Found: C, 73.0; H, 7.1; N, 6.2.

[Fe^{II}_2(OH)(Me$_3$CCO$_2$)$_2$(Me$_3$tacn)$_2$](OTf), 1-Me-OTf: Neat Me$_3$tacn (0.684 g, 4.00 mmol) was added to a colorless solution of Fe(OTf)$_2$·2CH$_3$CN (1.744 g, 4.00 mmol) in 6 mL of acetonitrile to give a dark purple solution. In a separate vial, triethylamine (835 uL, 6.00 mmol) was added to a slurry of pivalic acid (0.408 g, 4.00 mmol) in 3 mL of acetonitrile to give a colorless solution. These solutions were combined to give a dark yellow solution. Water (36 uL, 2.00 mmol) was added to the reaction mixture and the volume was reduced in vacuo to 2 mL and placed in the freezer. After several hours at −30 °C, off-white crystals of **1**-Me were collected by vacuum filtration, washed with diethyl ether, and dried in vacuo (1.053 g, 65%). Product was recrystallized from acetone by slow evaporation. Anal. Calcd for $C_{29}H_{61}F_3Fe_2N_6O_8S$: C, 42.34; H, 7.47; N, 10.22. Found: C, 42.2; H, 7.4; N, 10.1.

[$Fe^{II,III}_2$O(Me$_3$CCO$_2$)$_2$(Me$_3$tacn)$_2$](OTf), 2-Me-OTf: A colorless solution of MMNO (0.072 g, 0.612 mmol) in 15 mL of acetonitrile was added dropwise over 15 min to a stirred slurry of pale yellow **1**-Me (0.987 g, 1.22 mmol) in 5 mL of acetonitrile. The solution color was observed to change immediately upon addition of the oxidant from yellow to dark green. Reduction of the solvent volume *in vacuo* followed by addition of diethyl ether resulted in formation of **2**-Me as a dark green precipitate that was collected by vacuum filtration, washed with diethyl ether, and dried in vacuo (0.793 g, 81%). Product was recrystallized by addition of diethyl ether to a concentrated acetonitrile solution followed by cooling at −30 °C for several days. Anal. Calcd for $C_{29}H_{60}F_3Fe_2N_6O_8S$: C, 42.40; H, 7.36; N, 10.23. Found: C, 42.5; H, 7.2; N, 10.1.

[Fe^{III}_2O(Me$_3$CCO$_2$)$_2$(Me$_3$tacn)$_2$](OTf)$_2$, 3-Me-OTf: A colorless solution of sodium triflate (0.172 g, 1.00 mmol) in 2 mL of acetonitrile was added to a pale yellow solution of **1**-Me (0.823 g, 1.00 mmol) in 5 mL of acetonitrile to give a yellow solution. Dropwise addition of a colorless solution of MMNO (0.117 g, 1.00 mmol) to the stirred reaction mixture resulted in a red-brown solution. Addition of diethyl ether to the reaction mixture resulted in formation of **3**-Me as an orange-red powder that was collected by vacuum filtration, washed with diethyl ether, and dried in vacuo (0.589 g, 62%). Large dark red plates were obtained by recrystallization of the orange-red powder from acetone/diethyl ether at room temperature. Anal. Calcd for $C_{30}H_{60}Fe_2F_6N_6O_{10}S_2$: C, 37.74; H, 6.34; N, 8.80. Found: C, 38.6; H, 6.4; N, 9.6.

[Fe^{II}_2(OH)(CF$_3$CCO$_2$)$_2$(Me$_3$tacn)$_2$](OTf), 1-F-OTf: Neat Me$_3$tacn (0.684 g, 4.00 mmol) was added to a yellow solution of Fe(OTf)$_2$·2CH$_3$CN (0.872 g, 2.00 mmol) and Fe(CF$_3$CCO$_2$)$_2$ (0.516 g, 2.00 mmol) to give a greenish-purple solution. In a separate vial, triethylamine (278 uL, 2.00 mmol) was added to a solution of water (36 uL, 2.00 mmol) in 1 mL of acetonitrile to give a colorless solution, which when added to the greenish-purple reaction mixture formed a yellow solution that changed to green within 1 min. The volume of the reaction mixture was reduced in vacuo to 5 mL and placed in the freezer. After 24 h at −30 °C, yellow crystals of **1**-F were collected by vacuum filtration, washed with diethyl ether, and dried in vacuo (1.022 g, 65%). Anal. Calcd for $C_{23}H_{43}Fe_2F_9N_6O_8S$: C, 32.64; H, 5.12; N, 9.93. Found: C, 32.7; H, 4.9; N, 9.9.

Physical Methods. ^{1}H NMR spectra were recorded on a General Electric QE-PLUS 300 MHz, a Varian Inova 400, or a General Electric Omega-600 spectrometer in CD_3CN, CD_3COCD_3, or $CDCl_3$ and referenced to tetramethylsilane. ^{2}H NMR spectra were recorded on a General Electric Omega-600 spectrometer in CH_3CN and referenced to C_6D_6 (7.16 ppm). Electronic absorption spectra were collected on a Shimadzu UV-3101PC, UV−Vis−NIR scanning spectrophotometer. EPR spectra were collected on a Brüker ER 200D-SRC spectrometer equipped with an Oxford Instruments ESR 910 continuous flow cryostat. Unless otherwise indicated, the spectra were recorded at 10 K with a microwave power of 20 μW, a frequency of 9.65 GHz, a modulation frequency of 100 kHz, a modulation amplitude of 4 G, a time constant of 200 ms, a scan time of 200 s, and a receiver gain of 1.25×10^4.

Multifield saturation magnetization data were collected as described previously[25,26] using a Quantum Design superconducting susceptometer from 2 to 200 K at fixed fields ranging from 0.2 to 5.5 T. The saturation magnetization difference data (holder-corrected sample minus holder-corrected control) were fit using the simplex method to find the spin Hamiltonian parameter set yielding the minimum in the standard quality of the fit parameter, χ^2. The software package to carry out the data analysis is a product of WEB Research Co., Edina, MN.

The mass spectrometry experiments were performed on a JEOL SX102/SX102/E five sector mass spectrometer (configuration BE-BEE).[27] The ion source was a JEOL Generation 2 ESI source operated at 5kV. The solutions used were approximately 10−100 μM of the metal complex. To reduce the possibility of the needle oxidizing the metal complexes, the needle was maintained at ground potential, while the front entrance to the capillary in the source was used to apply the electrospray potential (approximately −2 to −3 kV). Use of the normal method of operation (needle with high voltage and the front of the capillary at the ground) did not affect the spectra for most of the compounds studied.

Crystallographic Studies. Crystals of **1**-Ph-OTf, **1**-Ph-BPh$_4$, **2**-Ph-OTf, **2**-Ph-BPh$_4$, **3**-Ph-OTf, and **3**-Ph-BPh$_4$ suitable for X-ray crystallographic analyses were obtained as described in the Experimental Section (vide supra). All crystals were coated with a viscous oil and mounted with super glue on the end of a glass fiber. The diffraction intensities of **1**-Ph-OTf and **2**-Ph-OTf were collected using Mo Kα̅ graphite monochromated radiation ($\lambda = 0.71073$ Å) on Siemens P4 and SMART single-crystal X-ray diffractometers, respectively, according to standard protocol. Data for all other crystals were collected on a Siemens P4/RA single-crystal X-ray diffractometer with Cu Kα̅ graphite monochromated radiation ($\lambda = 1.54178$ Å). The structures were solved either by direct methods or by Patterson interpretation and expansion (SHELXS-86) and difference Fourier methods, and refined by full-matrix least-squares methods (SHELXTL). All non-hydrogen atoms (other than the phenyl carbons of **1**-Ph-BPh$_4$ and **3**-Ph-OTf) were refined with anisotropic thermal parameters. The hydrogen on the bridging oxygen of **1**-Ph-OTf was located and its positional parameters were refined. All other hydrogen atoms were included using a riding model on the parent carbons with C−H bond distances fixed at 0.96 Å. The details of the data collection and refinement procedures are given in Table 1 and in the Supporting Information. Selected bond lengths and angles are given in Table 2.

Results and Discussion

Synthesis. Although tacn and Tp are effective ligands for μ-oxo-bridged diiron(III) aggregates, the low-spin iron(II) sandwich complexes, $[Fe(tacn)_2]^{2+}$ [28] and Fe(Tp)$_2$,[10] complicate their use in making model complexes of the reduced forms of non-heme proteins. It is possible to prepare a water-bridged complex, $[Fe_2(H_2O)(CF_3CO_2)_2(tacn)_2](CF_3CO_2)_2$ in CH_2Cl_2.[29]

(25) Day, E. P.; Kent, T. A.; Lindahl, P. A.; Münck, E.; Orme-Johnson, W. H.; Roder, H.; Roy, A. *Biophys. J.* **1987**, *52*, 837−853.
(26) Day, E. P. *Meth. Enzymol.* **1993**, *227*, 437−463.
(27) Strobel, F. H.; Adams, J. *J. Am. Soc. Mass Spectrom.* **1995**, *6*, 1232−1242.
(28) Boeyens, J. C. A.; Forbes, A. G. S.; Hancock, R. D.; Wieghardt, K. *Inorg. Chem.* **1985**, *24*, 2926−2931.
(29) Hagen, K. S. Unpublished.

Table 1. Crystallographic Data for $[Fe_2(OH)(Ph_3CCO_2)_2(Me_3Tacn)_2]^+$ (OTf^- Salt, 1-Ph-OTf; BPh^{4-} Salt, 1-Ph-BPh_4), $[Fe_2O(Ph_3CCO_2)_2(Me_3Tacn)_2]^+$ (2-Ph-OTf and 2-Ph-BPh_4), and $[Fe_2O(Ph_3CCO_2)_2(Me_3Tacn)_2]^{2+}$ (3-Ph-OTf and 3-Ph-BPh_4)

	1-Ph-OTf	**2**-Ph-OTf	**3**-Ph-OTf	**1**-Ph-BPh_4	**2**-Ph-BPh_4	**3**-Ph-BPh_4
empirical formula	$C_{63}H_{79}F_3Fe_2N_8O_8S$	$C_{63}H_{67}F_3Fe_2N_6O_9S$	$C_{64}H_{82}F_6Fe_2N_6O_{13}S_2$	$C_{84}H_{96}BFe_2N_7O_5$	$C_{84}H_{95}BFe_2N_7O_5$	$C1_{12}H_{119}B_2Fe_2N_8O_7$
fw	1277.10	1252.99	1433.18	1406.19	1405.18	1822.47
crystal system	monoclinic	orthorhombic	monoclinic	orthorhombic	orthorhombic	triclinic
T, °C	−100	−100	−100	−100	21	21
λ, Å	0.71073	0.71073	1.54178	1.54178	1.54178	1.54178
ρ_{calcd}, g cm^{-3}	1.175	1.352	1.436	1.262	1.245	1.229
abs. corr, μ, mm^{-1}	empirical, 0.567	empirical, 0.575	integration, 4.81	empirical, 3.589	empirical, 3.54	empirical, 2.83
space group, Z	$P2_1/c$, 4	*Pbca*, 8	$P2_1/c$, 4	*Pbca*, 8	*Pbca*, 8	$P\bar{1}$, 2
color of crystal	colorless	dark green	orange-red	colorless	dark green	orange-red
a, Å	17.254(4)	20.7008(3)	16.171(5)	20.4177(2)	20.5573(9)	12.937(2)
b, Å	15.452(5)	19.6161(1)	15.182(2)	19.2789(14)	19.3176(8)	14.977(3)
c, Å	24.427(6)	30.3179(5)	27.989(6)	37.6063(2)	37.7437(14)	25.627(5)
α, deg						93.84(1)
β, deg	106.28(1)		105.23(2)			91.12(1)
γ, deg						96.26(1)
V, Å^3	6251.63	12311.2	6630.2	14803.0	14988.7	4922.9
$R1$[a]	0.0604	0.0887	0.0802	0.0816	0.0716	0.0657
$wR2$[a]	0.1609	0.2261	0.1790	0.2153	0.1729	0.1758
GOF on F^2	1.038	1.165	1.020	1.021	1.022	1.015

[a] $R1 = \sum(|F_o| - |F_c|)/\sum(|F_o|)$, $wR2 = \sum[w(F_o^2 - F_c^2)^2/\sum w(F_o^2)^2]^{1/2}$ [$I > 2\sigma(I)$].

Table 2. Selected Bond Lengths (Å) and Angles (deg) for **1**, **2**, and **3** with Various Carboxylates and Counterions

complex (ref)	Fe···Fe	Fe(1)−O	Fe(2)−O	Fe(1)−N_c	Fe(1)−N_t	Fe(2)−N_c	Fe(2)−N_t	Fe−O−Fe	Fe−$N_{3\ plane}$	Fe(1) conf.[a] N−C−C−N[b]	Fe(2) conf.[a] N−C−C−N[b]
1-Me (OTf)[12a]	3.394 (3)	1.966 (3)		2.21 (1)	2.234 (6)			119.1 (3)	1.503	$\lambda\lambda\lambda$ −50 (1)	
1-Me (BPh_4)	3.474 (2)	1.996 (5)	2.000 (4)	2.22 (1)	2.232 (7)	2.22 (1)	2.233 (7)	120.8 (2)	1.48 1.49	$\lambda\lambda\lambda$ −51 (2)	$\lambda\lambda\lambda$ −48.7 (6)
1-F (OTf)[18]	3.400 (2)	1.97 (2)		2.219 (3)	2.250 (3)			119.2 (2)	1.508	$\lambda\lambda\lambda$ −50 (1)	
1-F (BPh_4)[12a]	3.477 (3)	1.997 (4)	1.999 (4)	2.218 (6)	2.232 (7)	2.22 (1)	2.233 (7)	120.8 (2)	1.48 1.49	$\lambda\lambda\lambda$ −49 (1)	$\lambda\lambda\lambda$ −51 (2)
1-H (ClO_4)[17]	3.32 (1)	1.987 (8)		2.26 (1)	2.30 (1)			113.2 (2)			
1-Ph (OTf)	3.414 (2)	2.008 (4)	2.002 (4)	2.270 (6)	2.288	2.29 (4)	2.261		1.56 1.57	$\lambda\lambda\lambda$ −50.1 (7)	$\delta\delta\delta$ 49.7 (5)
1-Ph (BPh_4)	3.424 (2)	2.007 (8)	2.002 (7)	2.27 (2)	2.236 (8)	2.28 (1)	2.269 (7)	117.3 (4)	1.55 1.56	$\lambda\lambda\lambda$ −23 (4)	$\delta\delta\delta$ 50 (2)
2-Ph (OTf)	3.123 (1)	1.847 (4)	1.800 (4)	2.24 (1)	2.307 (5)	2.26 (1)	2.314 (5)		1.56 1.57	$\delta\delta\delta$ 50 (2)	ddd/$\lambda\lambda\lambda$ −3 (4)
2-Ph (BPh_4)	3.155 (1)	1.818 (4)	1.844 (4)	2.25 (2)	2.314 (5)	2.26 (3)	2.309 (6)	119.0 (2)	1.57 1.58	$\delta\delta\delta$ 20 (4)	$\delta\delta\delta$ 34.6 (7)
2-Me (BPh_4)[39a]	3.158 (1)	1.881 (4)	1.853 (4)	2.253 (9)	2.299 (6)	2.245 (5)	2.322 (5)	115.5 (2)		$\lambda\lambda\lambda$ −31 (1)	$\lambda\lambda\lambda$ −37 (1)
3-Ph (OTf)	3.154 (2)	1.804 (7)	1.790 (7)	2.185 (9) 2.219 (9)	2.231 (9)	2.182 (9) 2.207 (8)	2.255 (9)	122.7 (4)	1.49 1.49	$\lambda\lambda\lambda$ −45.9 (2)	$\lambda\lambda\lambda$ −48 (2)
3-Ph (BPh_4)	3.160	1.796 (3)	1.792 (3)	2.188 (4) 2.213 (5)	2.245 (4)	2.185 (4) 2.192 (4)	2.249 (4)	123.4 (2)	1.49 1.49	$\delta\delta\delta$ 38 (2)	$\lambda\lambda\lambda$ −48 (1)

[a] The definitions of the λ and δ configurations are given in Figure S-7. [b] Average torsional angles are given for three Fe−N−C−C−N rings.

The alkylated tacn ligand, Me_3tacn, was introduced by Wieghardt to hinder the formation of the sandwich complex, $[Fe(Me_3tacn)_2]^{2+}$, and **1**-H was isolated in less than 50% yield from a 1:3:2.4 molar ratio of $Fe(ClO_4)_2 \cdot 4H_2O$, Me_3tacn, NaOAc in methanol after addition of an excess of $NaClO_4$.[16] A blue solution, which probably contains a small amount of the highly colored mixed valent dimer, $[Fe_2(OH)_3(Me_3tacn)_2]^{2+}$,[30] was reported to form before the NaOAc was added. Use of the bulkier *i*-Pr_3tacn or *i*-Bu_3tacn ligands affords five- and six-coordinate mononuclear high-spin iron(II) complexes, respectively.[31]

We find that the μ-hydroxo diiron(II) complexes with various bridging carboxylates are most conveniently prepared in high yield according to the stoichiometry of reaction 1. As it is important to use anhydrous iron(II) salts whose anions are less basic than the carboxylates that will subsequently be bound to the iron, we use iron(II) triflate as the iron source. The synthesis of iron(II) triflate as the anhydrous bis-acetonitrile solvate is convenient and the triflate salts of iron complexes are safer to handle than potentially explosive perchlorate salts. The stoichiometric nature of reaction 1 is particularly useful when ^{17}O or ^{18}O isotopically labeled hydroxide (generated stoichiometrically from H_2O and Et_3N) is required for spectroscopic analyses.

$$2\ Fe^{2+} + 2\ Me_3tacn + 2\ R_3CCOO^- + OH^- \rightarrow [Fe_2(OH)(R_3CCO_2)_2(Me_3tacn)_2]^+ \quad (1)$$

A 1:1 mixture of $Fe(OTf)_2 \cdot 2MeCN$ and Me_3tacn affords a purple

(30) Drueke, S.; Chaudhuri, P.; Pohl, K.; Wieghardt, K.; Ding, X.-Q.; Bill, E.; Sawaryn, A.; Trautwein, A. X.; Winkler, H.; Gurman, S. J. *J. Chem. Soc., Chem. Commun.* **1989**, 59−62.

(31) Diebold, A.; Elbouadili, A.; Hagen, K. S. *Inorg. Chem.* Submitted.

Scheme 1. Reactivity of $[Fe_2(OH)(O_2CR)_2(Me_3tacn_2]^+$ with Oxidants

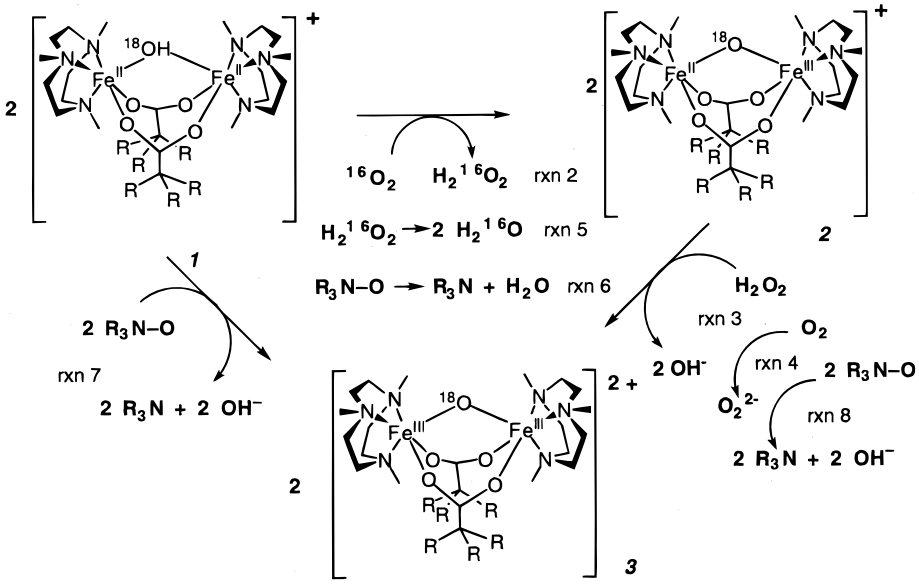

solution in acetonitrile. We have shown that this solution consists of an equilibrium mixture that contains some purple, low-spin $[Fe(Me_3tacn)(MeCN)_3]^{2+}$.[32] Addition of the carboxylate affords a solution containing only high-spin iron(II) complexes, and off-white crystals of **1**-Ph and **1**-Me are isolated in good yield following the addition of 1 equiv of hydroxide. Variation of the stoichiometry of reagents affords a series of mononuclear and binuclear iron(II) complexes that will be described elsewhere.[36b]

Reaction with Dioxygen. The oxidation of the original acetate-bridged complex, **1**-H, by dioxygen has been subjected to a kinetic analysis and a mechanism has been proposed.[16c,33] In our characterization of the solution behavior of **1** by NMR,[17] we noticed that exposure of an acetonitrile solution of the triflate salt of **1**-F to O_2 at room temperature affords an orange solution of the diiron(III) μ-oxo-bridged complex after a transient green solution is observed. Increasing the size of the carboxylate from trifluoroacetate to trimethylacetate and finally to triphenylacetate changes the reactivity of **1** and subsequent intermediates so as to afford green solutions that are sufficiently stable to allow crystallization of a green complex. Dark green crystals from the reaction of the triflate salt of **1**-Ph can be grown by adding diethyl ether to a concentrated acetonitrile solution followed by cooling to −25 °C. The green complexes are formulated as $[Fe_2O(R_3CCOO)_2(Me_3tacn)_2]^+$ (**2**) by single-crystal X-ray structures of the triphenylacetate and pivalate complexes, **2**-Ph and **2**-Me, as well as elemental analysis, NMR, electrospray mass spectroscopy, EPR, Mössbauer, and magnetic susceptibility data (*vida infra*).

The formation of **2** presumably takes place via reaction 2 in which H_2O_2 is a byproduct (Scheme 1). Complex **2** reacts further with either the H_2O_2 that was generated in reaction 2 or with the excess O_2 present in the solution to form the diiron(III) complex, **3**, according to reactions 3 and 4, respectively. To obtain pure samples of **2**-Ph in solution as well as in the solid state for physicochemical analyses, the conditions for its formation and isolation were optimized. Our initial approach was to use the BPh_4^- salt of **1**-Ph because it is considerably less soluble than the triflate salt and dark green crystals of **2**-Ph-BPh_4 separate from acetonitrile solution within minutes of their formation. However, since **2**-Ph-BPh_4 is isomorphous with **1**-Ph-BPh_4^-, mixtures of **1**-Ph and **2**-Ph are isolated unless it is assured that reaction 2 goes to completion. The reason that **2**-H, **2**-F, or **2**-Me may not have been prepared previously by reaction 2 is that subsequent oxidation via reactions 3 and 4 is too rapid.

$$2\,[Fe_2(OH)(R_3CCO_2)_2(Me_3tacn)_2]^+ + O_2 \rightarrow 2\,[Fe_2(O)(R_3CCO_2)_2(Me_3tacn)_2]^+ + H_2O_2 \quad (2)$$

$$2\,[Fe_2(O)(R_3CCO_2)_2(Me_3tacn)_2]^+ + H_2O_2 \rightarrow 2\,[Fe_2(O)(R_3CCO_2)_2(Me_3tacn)_2]^{2+} + 2\,OH^- \quad (3)$$

$$2\,[Fe_2(O)(R_3CCO_2)_2(Me_3tacn)_2]^+ + O_2 \rightarrow 2\,[Fe_2(O)(R_3CCO_2)_2(Me_3tacn)_2]^{2+} + O_2^{2-} \quad (4)$$

Other Oxidants. The excess of oxidizing equivalents in the byproduct of reaction 2, H_2O_2, that results in reaction 3, or the excess O_2 reagent in reaction 4, can be avoided by using hydrogen peroxide as an oxidant. The only byproduct is water, the terminally reduced form of oxygen (reaction 5). However, if H_2O_2(aq) is used, mechanistic considerations of the reactions may be complicated by a dilution of the $^{17}OH^-$ or $^{18}OH^-$ isotopic labels in **1**-Ph by exchange with excess water (*vida infra*). Therefore, we have utilized the anhydrous Dabco adduct of H_2O_2 that can be prepared as a somewhat stable solid.[24] Although freshly prepared Dabco·$2H_2O_2$ is a good source of H_2O_2, 2 equiv of H_2O are generated in reaction 5 and solid samples of the adduct are readily converted to the bis-*N*-oxide that can also oxidize either **1** or **2**. We have subsequently used trialkylamine *N*-oxides as oxidants for the synthesis of **2** since

(32) Blakesley, D.; Payne, S. C.; Hagen, K. S. *Inorg. Chem.* **2000**, *39*, 1979−1989.

(33) Liu, K. E.; Feig, A. L.; Goldberg, D. P.; Watton, S. P.; Lippard, S. J. *The Activation of Dioxygen and Homogeneous Catalytic Oxidation*; Barton, D. H. R., Martell, W. E., Sawyer, D. T., Eds.; Plenum Press: New York, 1993; pp 301−320.

(34) Chaudhuri, P.; Wieghardt, K. *Prog. Inorg. Chem.* **1987,** *35*, 329−436.

(35) Bossek, U.; Hummel, H.; Thomas, W.; Bill, E.; Wieghardt, K. *Angew. Chem., Int. Ed. Engl.* **1996**, *34*, 2642−2645.

(36) Payne, S. C. Ph.D. Thesis, Emory University, 1998. (b) Payne, S. C.; Blakesley, D.; Hagen, K. S. Unpublished.

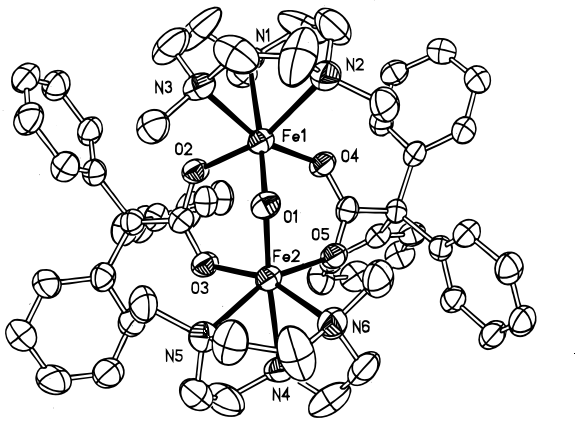

Figure 1. ORTEP (30% ellipsoids) of **2**-Ph as the BPh_4 salt. Hydrogen bonds omitted for clarity.

the only byproducts of reaction 6 are 1 equiv of water and the amine.

$$2\,\mathbf{1} + H_2O_2 \rightarrow 2\,\mathbf{2} + 2\,H_2O \tag{5}$$

$$2\,\mathbf{1} + R_3N{-}O \rightarrow 2\,\mathbf{2} + OH^- + R_3NH^+ \tag{6}$$

The reactions of **1**-Ph and **1**-Me with *N*-methylmorpholine *N*-oxide (MMNO) or H_2O_2 are considerably more rapid than those of **2**-Ph and **2**-Me with these reagents. Therefore, **2**-Ph and **2**-Me can be isolated in crystalline form in good yields. The MMNO (or H_2O_2) are apparently consumed in two one-electron-transfer steps to form 2 equiv of **2**-Ph rather than by the concerted two-electron reaction 7 that forms **3**-Ph, which would have to be followed by a comproportionation of **1**-Ph and **3**-Ph and loss of a proton to form **2**-Ph. In fact mixtures of pure **1**-Ph and **3**-Ph in the presence of base do not exhibit the characteristic color of **2**-Ph. A 1:1 molar ratio of MMNO and **1**-Ph initially affords a green solution of **2**-Ph that turns orange as **3**-Ph is generated according to reaction 8. The stepwise reactions 6 and 8 are equivalent to overall reaction 7.

$$\mathbf{1} + R_3N{-}O \rightarrow \mathbf{3} + OH^- + R_3N \tag{7}$$

$$2\,\mathbf{2} + R_3N{-}O + OH^- + R_3NH^+ \rightarrow 2\,\mathbf{3} + 2\,OH^- + 2\,R_3N \tag{8}$$

The use of MMNO allows us to prepare the less stable mixed valent complexes, **2**-Me and even **2**-F, that could not be isolated in our hands using reaction 2. Reaction of **1**-F with MMNO affords a green solution of **2**-F from which a small amount of **2**-F cocrystallizes with a substantially larger quantity of orange-red **3**-F. An extra equivalent of NaOTf is added to reactions designed to isolate **3** to replace the OH^-, HO_2^-, or O_2^{2-} byproduct counterions generated from the oxidants.

Crystal Structures. The crystal data for both the triflate and BPh_4 salts of the diiron(II) (**1**-Ph-OTf and **1**-Ph-BPh_4), the mixed valent iron(II)(III) clusters (**2**-Ph-OTf, **2**-Ph-BPh_4), and the diiron(III) clusters (**3**-Ph-OTf and **3**-Ph-BPh_4) are summarized in Table 1 and core metrical parameters of these and related structures are gathered in Table 2. The general structural type of two pseudo-octahedral metals bridged by an oxo or hydroxo group and two carboxylates and terminally capped by tridentate ligands is well established in iron as well as other transition metal chemistry (Figure 1).[34] Figures of all the structures are provided in the Supporting Information. A variable in these structures is the relative conformation of the five-membered $FeNCH_2CH_2N$ chelate rings that adopt either the $\lambda\lambda\lambda$ or $\delta\delta\delta$ conformation. Both carbon atoms in these rings lie on one side of the N−Fe−N plane but one is typically displaced 0.5 Å further from the plane than the other in well-behaved structures. The torsional angles of the N−C−C−N groups (N−C−C−N_{Torr}) in disorder-free tacn ligands approach 50° or −50° for δ and λ configurations, respectively. The large thermal parameters of the carbons on some of the rings are indicative of disorder that is also reflected in ring C−C bond lengths that are apparently less than 1.5 Å. In **1**-Ph-OTf, the tacn ligands have opposite conformations with N−C−C−N_{Torr} of −50.1° and 49.5° for the $\lambda\lambda\lambda$ and $\delta\delta\delta$ configurations, respectively. In **1**-Ph-BPh_4 one ring has N−C−C−N_{Torr} of 50° while the other is only −23° and in **2**-Ph-OTf one ring is well behaved (Table 2) but the carbon atoms of the other have very large thermal parameters and an N−C−C−N_{Torr} angle of −3°. Some of the dimers clearly have a pseudo-mirror plane through the bridging oxygen and carboxylate carbons that relate the $\lambda\lambda\lambda$ and $\delta\delta\delta$ configurations of the two tacn ligands. However, the macrocycle conformations in others are both either $\lambda\lambda\lambda$ or $\delta\delta\delta$ related by a pseudo-2-fold axis through the bridging oxygen. In **2**-Ph-OTf a mixture of both structures cocrystallize but there is clear disorder of only one of the tacn ligands. This may relate to the crystallization process from solution where there is rapid flipping of the conformers on the time scale of the NMR experiment (vide infra).

The structures of the clusters containing the smaller carboxylate substituents (**1**-H, **1**-F, **1**-Me) lie on crystallographically imposed 2-fold axes that pass through the bridging oxygen atom. However, both the triflate and BPh_4^- salts of **1**-, **2**-, or **3**-Ph have no crystallographically imposed symmetry. There is a distinct asymmetry in the propeller-like rotational conformation of the triphenylacetate substituents of **1**-Ph-OTf. Two of the phenyl rings on one carboxylate are syn and the third is anti with respect to the bridging oxo and the plane of the carboxylate group. The other carboxylate has two anti phenyl rings and one syn. The former arrangement exists in the five other structures presented here. The triphenyl groups on the carboxylates are related to each other by an approximate 2-fold axis through the bridging oxo. The orientation of the phenyl rings is most likely determined by packing interactions as there is free rotation of the triphenyl groups in solution as determined by NMR (vide infra).

A reasonably strong hydrogen bond exists between the bridging hydroxide of **1**-Ph and one oxygen atom of the triflate (O···OSO_2CF_3 3.17 Å), although the O···O interaction is longer than observed in the triflate salts of **1**-F (O···OSO_2CF_3 2.90 Å)[17] and **1**-Me (O···OSO_2CF_3 2.98 Å).[12a] The Fe···Fe separation of 3.414(2) Å is similar to those found in **1**-F and **1**-Me, but considerably greater than the 3.32 Å found in **1**-H. The Fe−$O_{carboxylate}$ bonds average to 2.12(1) Å and the Fe−N distance average to 2.28(2) Å. There is no distinction of the Fe−N bond trans to the bridging hydroxide.

Mixed Valent Structures. The only difference in atom composition between **1** and **2** is the loss of the proton on the bridge as there is still one counterion associated with **2**-Ph. The hydrogen bond that exists in the triflate salt of **1** cannot form in **2**-Ph-OTf, which crystallizes in a different crystal system than **1**-Ph-OTf. The shortest distance between a triflate oxygen and the bridging oxygen in **2**-Ph-OTf is 5.85 Å. Since no hydrogen bond exists in **1**-Ph-BPh_4, there is little change on oxidation, and both **1**-Ph-BPh_4 and **2**-Ph-BPh_4 are isomorphous. One must rely on a spectroscopic technique such as NMR (vide infra) to ensure that a sample of **2**-Ph-BPh_4 is not contaminated

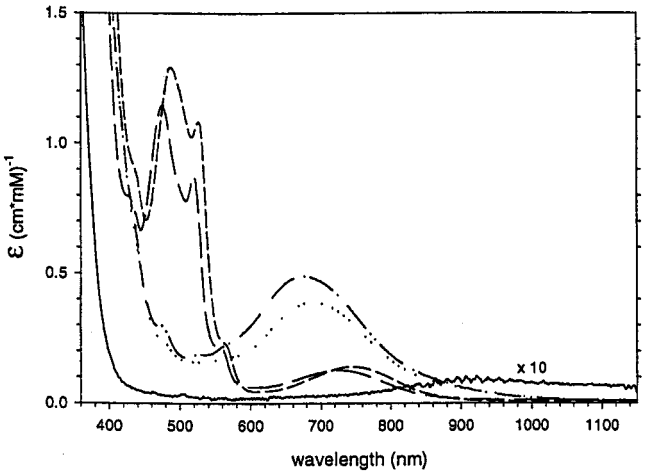

Figure 2. Visible spectra of **1**-Ph (×10), **2**-Ph (− · −), **3**-Ph (- - -), **2**-Me (···), and **3**-Me (− −) (2.0 mM in CH_3CN).

with the diiron(II) complex. The assignment of the bridge as an oxide is supported by Fe−O distances (1.800(4) and 1.847(4) Å in **2**-Ph-OTf and 1.818(4) and 1.844(4) Å in **2**-Ph-BPh_4) that are similar to those in diiron(III) μ-oxo dicarboxylato-bridged complexes (1.77−1.80 Å) and are considerably shorter than those in **1**-Ph (1.97−2.01 Å). Although the bonding interactions of the two iron atoms are very similar, bonds to one of the irons are consistently shorter than the bonds to the other iron. However, both sets of distance values are very similar to those in **3** and dramatically shorter than those in **1**. The Fe−O bonds (1.961(5) and 2.005(5) Å) in the hydroxy-bridged mixed valent complex, $[Fe_2(OH)(O_2CCMe_3)_2(Me_3tacn)_2](ClO_4)_2$, **4**-Me($ClO_4$),[35] are more similar to those in **1** than in **2.** This trend also applies to the Fe···Fe distance of 3.400(3) Å in **4**-Me-ClO_4, which is similar to that in **1**-Ph-OTf (3.414(2) Å) and **1**-Ph-BPh_4 (3.424(2) Å), but is considerably longer than the Fe···Fe distances in **2**-Ph-OTf (3.123(1) Å) and **2**-Ph-BPh_4 (3.155(1) Å). The nature of the bridging ligand clearly plays a more significant role in determining the core dimensions than does the oxidation state of the irons. The triflate salts of **1**-Me and **4**-Me cocrystallize in the same lattice.[36] The two irons in **2**-Ph are not crystallographically related by symmetry, yet their similar environments suggest either a disordered distribution of Fe(II) and Fe(III) or a delocalized, Class III, mixed valent complex as found in the solid-state structure of $[Fe_2(OH)_3(Me_3tacn)_2]^{2+}$.[37]

Electronic Absorption Properties. The visible absorption spectra for all complexes isolated are shown in Figure 2 and their data are tabulated in Table 3. The colorless diiron(II) complexes are characterized by an absorption in the UV and a weak absorption in the near-IR region at 900 nm ($\epsilon = 10$ M^{-1} cm^{-1}). The spectra of the green mixed valent complexes are dominated by absorption maxima at 685 ($\epsilon = 435$ M^{-1} cm^{-1}), 674, and 695 nm, for **2**-Ph, **2**-Me, and **2**−F, respectively. This absorption is likely a result of intervalence charge transfer, similar to that observed in the exchange-coupled mixed valent diiron(II,III) complex, $[Fe_2(OH)_3(Me_3tacn)_2]^{2+}$ (740 nm, $\epsilon \sim$ 5,700 M^{-1} cm^{-1}).[38] Other weaker features occur at 475 (306), 529 (200), and 564 nm (208 M^{-1} cm^{-1}). The diiron(III) complex has much more intense features in this region (487 (1300), 527 (1100), and 565 (sh)) and a broad feature at 745 nm (140) that is weaker than the 685 nm feature of **2**. These spectral differences afford us with a convenient method to monitor the reaction sequence of **1** with O_2 and other oxidants.

Table 3. Visible Absorption Data for **1**-, **2**-, and **3**-Ph-OTf and **2**- and **3**-Me-OTf

	CH_3CN: λ (ϵ)	CH_2Cl_2: λ (ϵ)	THF: λ (ϵ)
1-Ph-OTf	906 (10)		
2-Ph-Otf	685 (390)	688 (390)	687 (380)
	566 (sh)	566 (sh)	566 (sh)
	525 (170)	525 (170)	526 (170)
	476 (sh)	476 (sh)	476 (sh)
2-Me-OTf	673 (490)	674 (520)	671 (510)
	525 (sh)	526 (sh)	527 (sh)
	475 (300)	476 (310)	476 (300)
3-Ph-OTf	745 (140)	745 (160)	745 (120)[a]
	567 (sh)	567 (sh)	567 (sh)
	527 (1100)	527 (1200)	527 (850)
	487 (1300)	486 (1500)	491 (1000)
3-Me-OTf	725 (130)	728 (130)	729 (120)
	559 (230)	556 (220)	559 (810)
	520 (880)	521 (940)	478 (1100)
	476 (1100)	476 (1200)	431 (sh)
	428 (sh)	428 (sh)	

[a] **3**-Ph-OTf is less soluble in THF, therefore <2mM solution.

Table 4. Multinuclear NMR of Triflate Salts in Acetonitrile, ^1H (^2H), δ/ppm[a]

	1-Ph	**1**-Me	**2**-Ph	**2**-Me	**3**-Ph	**3**-Me
CH_3	55.5 (55.2)	71.2 (70.3)	(23.8)	(18.3)	(27.6)	(21.2)
	41.4 (40.4)	31.1 (30.8)	(16.1)	(12.5)	(19.7)	(14.4)
CH_2	74.9	72.8	29.2*	27.4*	26.0*	26.0*
	70.0	64.1	28.3*	19.6*	22.3*	22.1*
	64.3	61.7	19.4*	18.1*	16.6*	16.7*
	53.6	54.8	17.6*	12.4*	14.5*	14.9*
	29.2	32.3	12.9*	7.2*	12.9*	13.3*
	17.3	8.0	11.4*			8.2*
R	8.9	11.5	8.0	3.9	7.5	3.1
	7.1		7.4		7.2	
	6.3		7.1			

[a] Resonances with an asterisk have not been assigned.

When 2.0 mM acetonitrile solutions of **1**-Me and **1**-Ph are treated with an excess of O_2 green solutions of **2** form that reach maximum intensity at 674 nm within 3 min for **2**-Me and at 685 nm within 15 min for **2**-Ph. These reactions are followed by a slower conversion to orange solutions of **3** (Figures 3 and S9).

The μ-hydroxo-bridged mixed valent complexes **4**-Me and **4**-Ph[36] are essentially featureless between 600 and 900 nm where the dominant feature in the spectrum of **2** occurs. Rather, a weak broad band appears in the NIR spectrum of **4** at 1350 nm ($\epsilon \sim$ 60 M^{-1} cm^{-1}), which has been assigned as the intervalence band[35] analogous to the 1350 nm feature in $[Fe_2BPMP(O_2CR)_2]^{2+}$.[11c] Complex **2** is featureless in this region and reactions of **1** with O_2 only show a decrease in the NIR band of **1** and no indication that **4** is an intermediate. This reaction pathway is better demonstrated by NMR and EPR spectroscopy, and mass spectrometry.

NMR Studies. The isotropic shifts of resonances of ligands associated with the paramagnetic metal ions afford well-resolved, although broad, spectra for the diiron(II) complexes (Table 4). We have demonstrated that subtle changes in structure of diiron(II) complexes are readily detected by NMR.[14,15] ^1H NMR spectra of **1** reflect the effective molecular C_{2v} symmetry obtained by rapid interconversion of the $\lambda\lambda\lambda$ and $\delta\delta\delta$ conformations of the Me_3tacn ligand on the NMR time scale. These spectra are useful for establishing purity and are readily distinguished from those of other iron(II) complexes such as

(37) Gamelin, D. R.; Bominaar, E. L.; Kirk, M. L.; Wieghardt, K.; Solomon, E. I. *J. Am. Chem.* Soc. **1996**, *118*, 8085−8097.

(38) Gamelin, D. R.; Bominaar, E. L.; Mathoniere, C.; Kirk, M. L.; Wieghardt, K.; Girerd, J. J.; Solomon, E. I. *Inorg. Chem.* **1996**, *35*, 4323−4335.

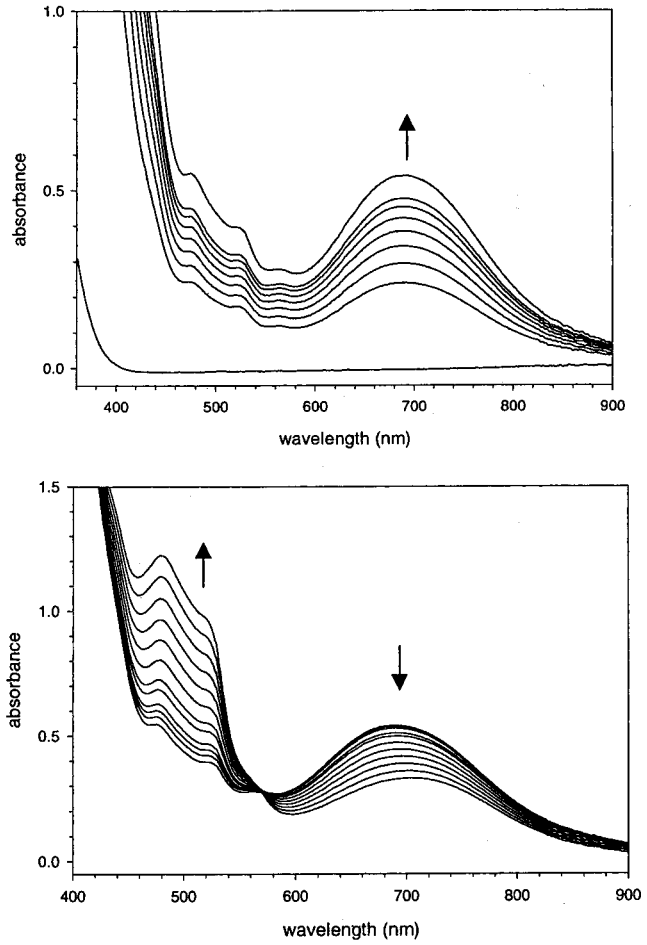

Figure 3. Visible spectra of the reaction of **1**-Ph-OTf (2.0 mM in CH_3CN) with dioxygen. Top panel shows the maximum formation of **2**-Ph-OTf. Bottom panel shows the continuation of reaction; conversion of **2**-Ph-OTf to **3**-Ph-OTf with all spectra taken at 30 min intervals.

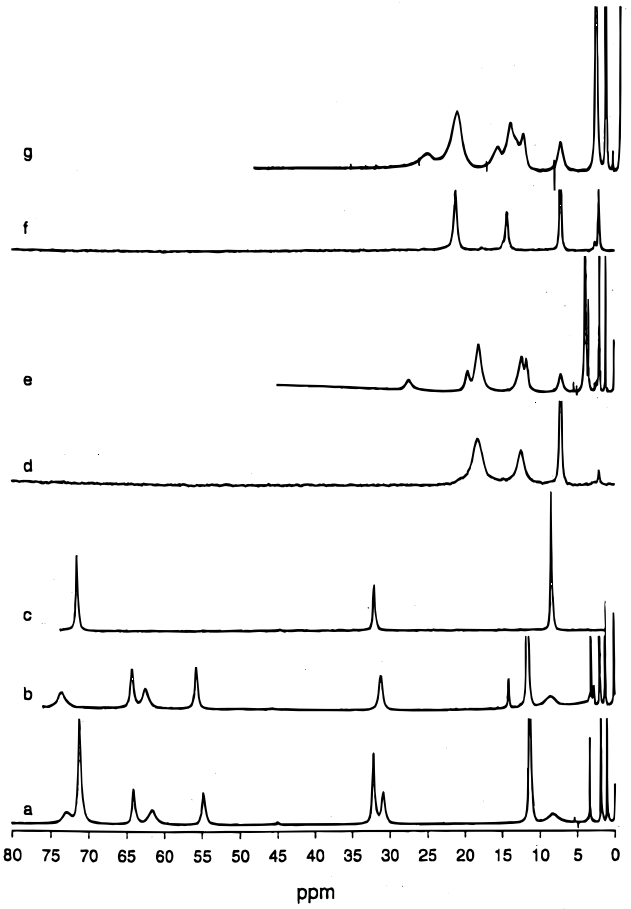

Figure 4. ^1H NMR spectra (in CD_3CN, reference TMS, 500 MHz) and ^2H NMR spectra (in CH_3CN, reference C_6D_6, 92 MHz) of **1**-, **2**-, and **3-Me-OTf**: (a) ^1H/**1**-Me-OTf, (b) ^1H/**1**-D-Me-OTf, (c) ^2H/**1**-D-Me-OTf, (d) ^2H/**2**-Me-OTf, (e) ^1H/**2**-Me-OTf, (f) ^2H/**3**-D-Me-OTf, and (g) ^1H/**3**-Me-OTf.

$[Fe_2(OH)(R_3CCOO)(OTf)(Me_3tacn)_2]^+$, $[Fe_2(OH)(OTf)_2(Me_3tacn)_2]^+$, $[Fe(R_3CCOO)(Me_3tacn)]^+$, $[Fe(H_2O)(R_3CCOO)(Me_3tacn)]^+$, and $[Fe(Me_3tacn)(CH_3CN)_3]^{2+}$, all of which we have independently prepared using variations in the stoichiometry of reagents used to prepare **1**.[32,36b] The spectra are characterized by eight isotropically shifted resonances for the Me_3tacn ligands and one or three resonances for the carboxylate, in **1**-Me and **1**-Ph, respectively (Figures 4 and 5). Unique H in C_{2v} symmetry: **1**-Ph: Me (6H) 55.5, Me (3H) 41.4, $3CH_2$ (1H each) 75.2, 70.4, 64.8, 53.6, 29.2, and 17.2, *o*-H 8.9, *m*-H 7.1, *p*-H 6.3 ppm downfield of TMS. ^{19}F NMR spectroscopy is particularly useful for assessing the purity of trifluoroacetate- and triflate-bridged complexes.

Only two species are initially detected when the reaction between **1** and dioxygen is monitored by ^1H NMR. The Me_3CCOO^- resonance in **1**-Me at 11.5 ppm decreases in intensity while that of **2**-Me at 3.8 ppm increases. That resonance subsequently diminishes as that of the orange **3**-Me at 3.3 ppm grows in. The Ph_3CCOO^- resonances of **1**-Ph at 8.9, 7.1, and 6.3 ppm decrease during the reaction with O_2, while those of **2**-Ph at 7.9, 7.4, and 7.0 ppm increase and then decrease to a set of incompletely resolved resonances at 7.5, 7.2 ppm. The large line widths and low resolution observed for the Me_3tacn ligands in **2** and **3** are similar to other μ-oxo-bridged diiron(III) complexes,[23,39−41] and make species identification and signal assignments difficult. However, the broad resonances associated with the slow electron relaxation of **2** and **3** can be overcome by observing a nucleus such as deuterium that has a lower nuclear magnetogyric ratio.[42] We have therefore analyzed the spectra of complexes prepared with the ligand deuterated at the methyl groups, $(CD_3)_3$tacn.

Two ^2H resonances are observed at 55.0 and 40.1 ppm for **1**-Ph, at 18.5 and 10.7 ppm for **2**-P**h,** and at 22.1 and 14.2 ppm for **3**-Ph (Figure 5). The widths of the ^2H resonances of **2** and **3** are the same as those of **1,** in marked contrast to the poorly resolved ^1H NMR spectra of **2** and **3**. The two resonances are consistent with maintenance of the solid-state structures in solution and an equivalence of the two irons of the mixed valent **2** on the time scale of the NMR experiment. On the basis of the intensities, the more downfield shifted resonance for each complex corresponds to the four $N-CH_3$, cis to the bridging oxo/hydroxo, and the other resonance is of the two $N-CH_3$ lying on the pseudo molecular mirror plane containing the iron atoms. This behavior has been attributed to the trans effect of the bridging oxo group.[39] Since the isotropic shifts are pre-

(39) Wu, F.-J.; Kurtz, D. M., Jr. *J. Am. Chem. Soc.* **1989**, *111*, 6563−6572.

(40) Armstrong, W. H.; Spool, A.; Papaefthymiou, G. C.; Frankel, R. B.; Lippard, S. J. *J. Am. Chem. Soc.* **1984**, *106*, 3653−3667.

(41) Norman, R. E.; Yan, S.; Que, L., Jr.; Backes, G.; Li, J.; Sanders-Loehr, J.; Zhang, J. H.; O'Conner, C. J. *J. Am. Chem. Soc.* **1990**, *112*, 1554−1562.

(42) LaMar, G. N.; Horrocks, W. D.; Holm, R.H., Eds. *NMR of Paramagnetic Molecules*; Academic Press, Inc.: New York, 1973. (b) Bertini, I.; Luchinat, C. *NMR of Paramagnetic Molecules in Biological Systems*, 3rd ed.; Bertini, I., Luchinat, C., Eds.; Benjamin/Cummings Publishing Co.: Reading, MA, 1986. (c) Bertini, I.; Luchinat, C. NMR of Paramagnetic Substances. *Coord. Chem. Rev.* **1996**, *150*, 77−110.

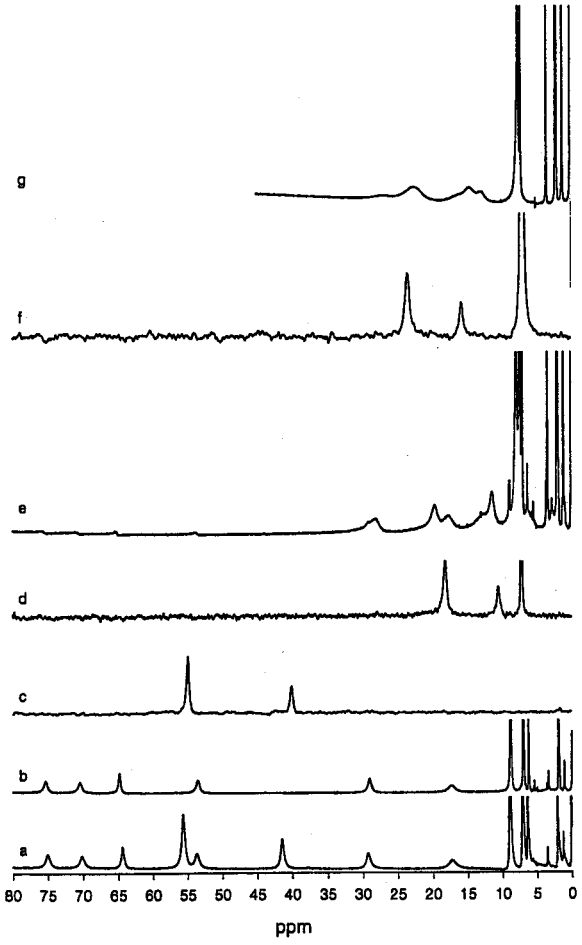

Figure 5. ^{1}H NMR spectra (in CD_3CN, reference TMS, 500 MHz) and ^{2}H NMR spectra (in CH_3CN, reference C_6D_6, 92 MHz) of **1**-, **2**-, and **3-Ph-OTf**: (a) ^{1}H/**1**-Ph-OTf, (b) ^{1}H/**1**-D-Ph-OTf, (c) ^{2}H/**1**-D-Ph-OTf, (d) ^{2}H/**2**-Ph-OTf, (e) ^{1}H/**2**-Ph-OTf, (f) ^{2}H/**3**-D-Ph-OTf, and (g) ^{1}H/**3**-Ph-OTf.

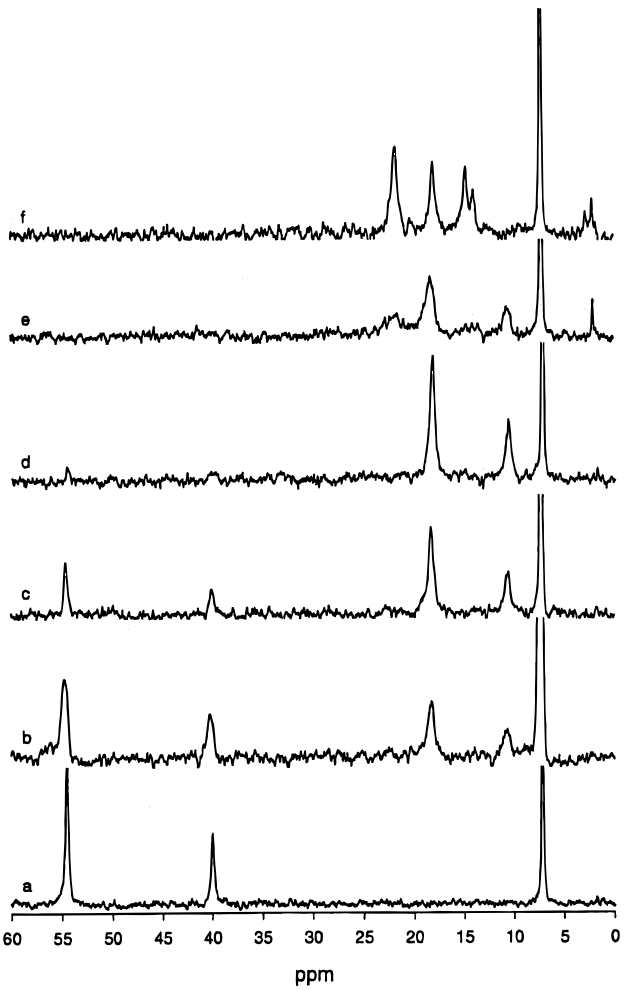

Figure 6. ^{2}H NMR spectra (in CH_3CN, reference C_6D_6) following the reaction of **1**-Ph-OTf with dioxygen over time.

dominately contact in origin, the longer $Fe-N_{trans}$ bonds convey less of the unpaired spin density of the irons to the *trans*-methyls than to the *cis*-methyls. The isotropic shifts of **2** are actually smaller than those of **3** despite the larger paramagnetism of **2** ($S = {}^1/_2$ ground state) than of **3** ($S = 0$ ground state). This is indicative of comparable electronic exchange coupling between the two irons which has been confirmed by magnetic susceptibility (vide infra). The isotropic shifts of the more weakly coupled μ-hydroxy-bridged complex **4**-Me[36] or phenoxy-bridged Fe(II)Fe(III) complexes, ($[Fe^{II}Fe^{III}(bimp)(O_2CPh)_2]^{2+}$ [43] and $[Fe^{II}Fe^{III}(bpmp)(O_2CEt)_2]^{2+}$ [11c]) are even larger than those of **1**-Me. Sharp, highly shifted resonances are also seen in a weakly coupled octanuclear iron(III) μ_3- and μ_4-oxo-bridged complex, $[Fe_8O_5(OAc)_8(tren)_4]^{5+}$.[12b,44] The μ-hydroxo diiron(III) complex, $[Fe_2(OH)(O_2CCH_3)_2(HBpz_3)_2]^+$, has highly shifted, although broad, resonances as well.[45]

The ^{2}H NMR spectra of the reaction mixture of **1**-Ph with O_2 (Figure 6) shows a decrease in intensity of the two resonances of **1**-Ph at 55 and 40 ppm along with the appearance of the resonances of **2**-Ph at 18 and 11 ppm. No resonances of **4**-Ph are seen in dry solvents. Only after **1**-Ph has been completely consumed are resonances of **3**-Ph at 22 and 14 ppm seen. The small shift in the final resonances of **2**-Ph is possibly due to interaction with the OH^- byproduct of the reaction. Analogous spectra for the reaction of **1**-Me with O_2 are depicted in Figure 7. Two resonances appear at identical isotropic shifts to those of pure **2**-Me, but then gradually shift downfield until the final two resonances are seen at 21.2 and 14.4 ppm, which correspond to those of **3**-Me. An electron self-exchange reaction between **2**-Me and **3**-Me, which is rapid on the NMR time scale under these conditions, causes this averaging of resonances. This is in contrast to the observation of distinct pivalate resonances of **2**-Me and **3**-Me that were observed with ^{1}H NMR (vide supra). An analysis of the proton and electron-transfer reactions of these complexes will be presented in a separate report.[36]

Mass Spectrometry. Continuous-introduction electrospray ionization mass spectroscopy (ESI-MS) is a useful technique not only for identifying coordination complexes and transient species that exist in solution,[46] but also for real time monitoring of reactions.[47] The ESI-MS spectra of acetonitrile solutions of complex **1**-Ph (Figure 8) are remarkably clean, and show signals at *m*/*z* 1047 for $[Fe_2(^{18}OH)(Ph_3CCO_2)_2(Me_3tacn)_2]^+$ and at 876 for loss of one of the Me_3tacn ligands in $[Fe_2(^{18}OH)(Ph_3CCO_2)_2(Me_3tacn)]^+$. Reaction with $^{16}O_2$ or MMN^{16}O affords peaks at *m*/*z* 1046 and 875, or loss of one mass unit while

(43) Mashuta, M. S.; Webb, R. J.; Mccusker, J. K.; Schmitt, E. A.; Oberhausen, K. J.; Richardson, J. F.; Buchanan, R. M.; Hendrickson, D. N. *J. Am. Chem. Soc.* **1992**, *114*, 3815−3827.

(44) Nair, V. S.; Hagen, K. S. *Inorg. Chem.* **1994**, *33*, 185−186.

(45) Turowski, P. N.; Armstrong, W. H.; Liu, S. C.; Brown, S. N.; Lippard, S. J. *Inorg. Chem.* **1994**, *33*, 636−645.

(46) Kim, J.; Dong, Y.; Larka, E.; Que, L., Jr. *Inorg. Chem.* **1996**, *35*, 2369−2372.

(47) Lee, E. D.; Mück, W.; Henion, J. D.; Covey, T. R. *J. Am. Chem. Soc.*, **1989**, *111*, 4600−4604.

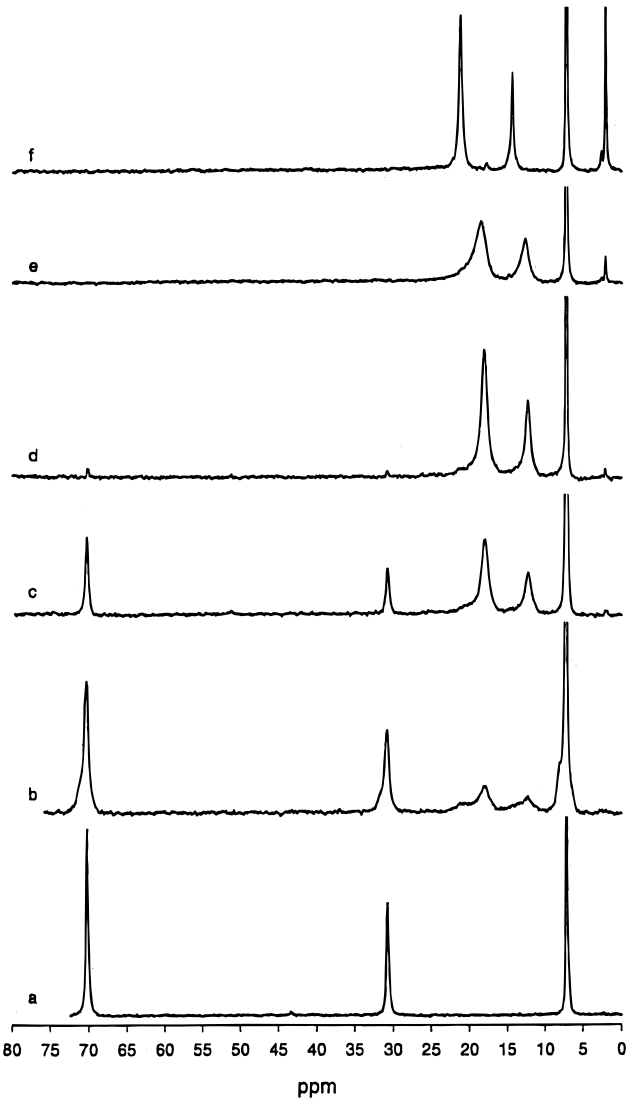

Figure 7. ^{2}H NMR spectra (in CH_3CN, reference C_6D_6) following the reaction of **1**-Me-OTf with dioxygen over time.

maintaining a monopositive charge. This corresponds to the loss of the proton of the μ-OH^- and one electron to form the $Fe^{II}-{}^{18}O-Fe^{III}$ unit in **2**-Ph. The isotope distribution pattern (Figure 8 inset) does not change when either natural abundance $^{16}O_2$ or MMN^{16}O are used as oxidants. Crystalline samples isolated from acetonitrile solutions also maintain the ^{18}O enrichment, confirming our earlier resonance Raman studies that indicate that the reaction takes place by an outer-sphere reaction.[20] The byproducts of reactions 2 and 3, H_2O_2 and OH^-, do not exchange with the bridge within the time required to isolate the crystalline product. The spectrum of isolated **3**-Ph has peaks at *m*/*z* of 1193 and 522 for {**3**-Ph-OTf}$^+$ and {**3**-Ph}$^{2+}$, respectively. These peaks did not appear during the reaction of **1**-Ph with O_2 over a 30 min period at room temperature indicating that the reaction had stopped at **2**-Ph.

Samples of **1**-Me in acetonitrile that have been partially enriched in ^{18}O show *m*/*z* peaks at 673, 675 and 502, 504 for μ-^{16}OH and μ-^{18}OH cations and the loss of one Me_3tacn ligand, respectively (see Figure S10). On oxidation with $^{16}O_2$ the peaks appear at *m*/*z* 672, 674, 501, and 503 corresponding to the mixed valent μ-oxo **2**-Me. Unlike for the reaction with **1**-Ph, a small amount of **3**-Me with peaks at 821 and 823 for {**3**-Me-OTf}$^+$ appears in the reaction of **1**-Me with O_2, but not in samples prepared from purified, crystalline **2**-Me. Intermediates of other

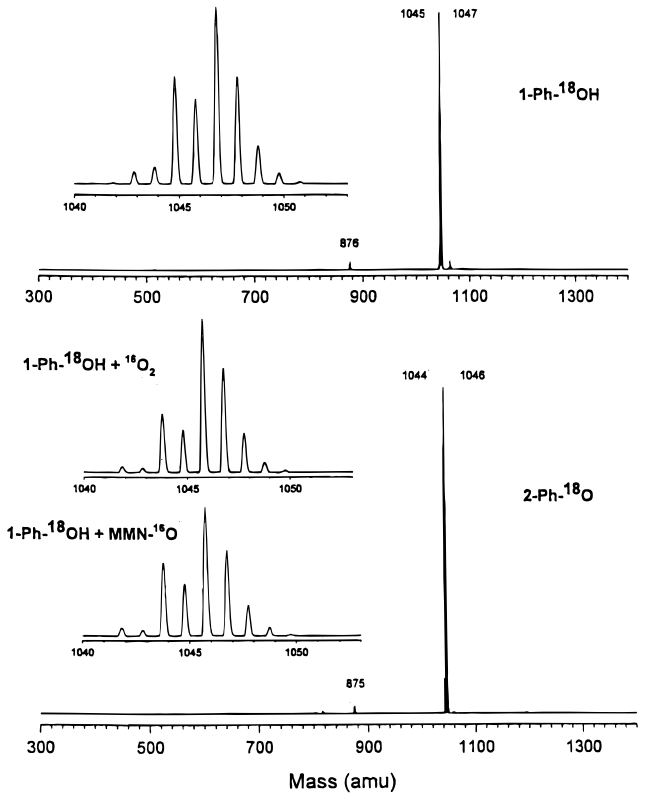

Figure 8. ESI-mass spectra of 20 M solutions of **1**-Ph-^{18}OH and **2**-Ph-^{18}O.

mass, especially peroxo-bound dinuclear and tetranuclear complexes, were looked for, but were not detected. The time course of the reaction can be monitored by following the drop in intensity of the 673 peak and growth of the 672 peak as **1**-Me is converted to **2**-Me.

EPR Studies. Frozen acetonitrile solutions (2.0 mM) of analytically pure **2**-Ph and **2**-Me exhibit a rhombic signal at $g = 1.97$, 1.93, and 1.90 at 10 K that integrates to 1.12 and 1.11 spins per dimer, respectively (relative to a 3.076 mM aqueous solution of CuEDTA, Figure 9). This g value of less than 2.0 is characteristic of an antiferromagnetically coupled Fe(II)Fe(III) mixed valent species with an $S = {}^1/_2$ ground state.[48] The spectra are observed at temperatures as high as 85 K indicating that there is no facile mechanism for electron relaxation. Acetonitrile solutions of **1**-Ph treated with O_2 and frozen after 10 min exhibit a rhombic signal at $g = 1.97$, 1.93, and 1.90. After 2 h at room temperature, the refrozen solution exhibited an axial signal identical with that of **2**-Ph. The same behavior was observed with **1**-Me and O_2 or when NMMO was used as the oxidant. These spectra are similar to that of **2**-H which was generated by controlled-potential electrolysis of **3**-H,[16b] but quite distinct from the hydroxy-bridged Fe(II)Fe(III) complex, **4**-Me, which has a rhombic spectrum with $g_1 = 1.95$, $g_2 = 1.52$, and $g_3 = 1.43$.[35] Other μ-oxo-bridged diiron(III) complexes give slightly axial or rhombic spectra when reduced either electrochemically or radiolytically.[49,50] Thus it is clear that when reaction 2 is carried out in aprotic solvents, not enough of **4** is accumulated to be detected by either NMR or EPR and that proton transfer to the dioxygen is not the rate-limiting step.

(48) Bertrand, P.; Guigliarelli, B.; More, C. *New J. Chem.* **1991**, *15*, 445−454.

(49) Nivorozhkin, A. L.; AnxolabehereMallart, E.; Mialane, P.; Davydov, R.; Guilhem, J.; Cesario, M.; Audiere, J. P.; Girerd, J. J.; Styring, S.; Schussler, L.; Seris, J. L. *Inorg. Chem.* **1997**, *36*, 846−853.

(50) Davydov, R. M.; Menage, S.; Fontecave, M.; Graslund, A.; Ehrenberg, A. *J. Bio. Inorg. Chem.* **1997**, *2*, 242−255.

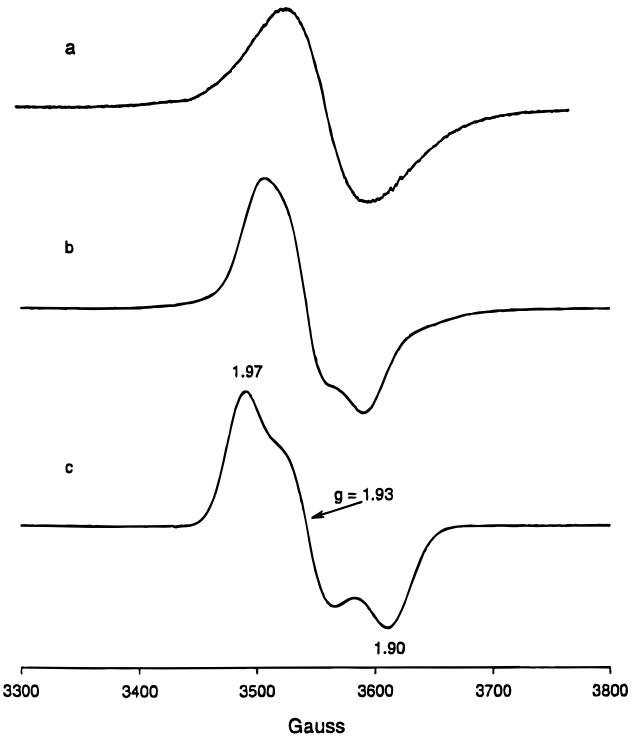

Figure 9. EPR spectra of 2.0 mM solutions of (a) **1**-Me-OTf and O_2 in MeCN, (b) pure **2**-Me-OTf, and (c) pure **2**-Ph-OTf in 1:1 MeCN/toluene.

Magnetism. The similarity in isotropic shifts in the NMR spectra of **2** and **3** suggests that the strong antiferromagnetic coupling that is well-known for μ-oxo-bridged diiron(III) also exists in the μ-oxo-bridged mixed valent cluster. This has been confirmed by multifield saturation magnetization experiments on **2**-Ph and **2**-Me. The data for **1**-Ph collected at five fields are fit to two equivalent high-spin Fe(II) sites with $D = 2.823$, $g = 2.00$, and $J = -12.1$ cm^{-1} and a χ^2 value of 1.7 for $H = -2JS_1 \cdot S_2$. The data for **2**-Ph collected at five fields are fit to an $S = {}^1/_2$ ground state with a high-spin Fe(III) site with $D = 1.46$ and $g = 2.00$, and a high-spin Fe(II) site with $D = 13.93$, E/D 0.285, $g = 2.069$, $J = -144$ cm^{-1}, and a χ^2 value of 5.9. The data for **2**-Me collected at five fields are fit to an $S = {}^1/_2$ ground state with a high-spin Fe(III) site with $D = 2.39$ and $g = 2.00$ and a high-spin Fe(II) site with $D = -11.42$, $g = 2.041$, $J = -119$ cm^{-1}, and a χ^2 value of 7.9. These unusually high values of J for **2**-Ph and **2**-Me are similar to those of μ-oxo-bridged diiron(III) complexes, $J = -119$ cm^{-1} for **3**-H[16b] and -111 cm^{-1} for **3**-Me,[35] and much greater than that observed for μ-hydroxo-bridged diiron(II), **1**-H $J = -13$ cm^{-1},[16b] or μ-hydroxo bridged mixed valent complex, **4**-Me $J = -12.9$ cm^{-1},[35] diiron(III), or μ-alkoxo-bridged mixed valent iron(II) iron(III) species.

Mössbauer. The characterization of **2** as a class II mixed valent species was first suggested by the resonance Raman data[20] and is now supported by Mössbauer data collected at 4.2 K. Although the quadrupole doublets are poorly resolved the spectrum can be fit to an intermediate relaxing species with Fe(II) and Fe(III) sites having $\delta = 1.09$, 0.6, $\Delta E_Q = 2.45$, 2.35, and $\Gamma = 0.55$, 0.75 mm s^{-1}, respectively (Figure 10).[51] The quadrupole splitting of the Fe(III) site is considerably larger than that seen for any other binuclear six coordinate high-spin iron(III) complexes, indicating a highly asymmetric electric charge distribution at the iron sites.[52] It is even higher than that observed in the class III valence-delocalized Fe(II)Fe(III) dimer, $[Fe_2(OH)_3(Me_3tacn)_2]^{2+}$.[53]

(51) For measurements made at 4.2 K and referenced to iron metal at room temperature. The relative areas are 53% to 40% indicating that a diiron(II) impurity (13%) is present in the sample.

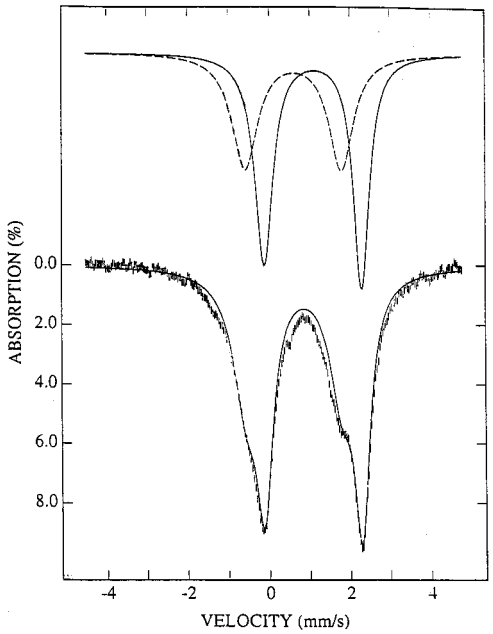

Figure 10. Mössbauer spectrum of a solid sample of **2**-Ph-OTf collected at 4.2 K.

Conclusion

Increasing the size of the carboxylates in the diiron(II) complex **1** and performing reactions in aprotic solvents has enabled us to trap a mixed valent intermediate **2** in reactions of **1** with dioxygen in aprotic solvents that otherwise give the diiron(III) complex **3**. The bulkier carboxylates and aprotic solvents can prevent or hinder the carboxylate shifts that have been proposed for inner-sphere reaction mechanisms.[16c,33] Substituting alternate oxidants, Dabco·$2H_2O_2$, and MMNO affords still cleaner reactions as the oxygen byproducts are fully reduced. All reagents react in a similar manner in aprotic solvents, as ESI-MS as well as resonance Raman studies[20] demonstrate that the labeled OH bridge is not exchanged by oxidant oxygen. This implies that an outer-sphere reaction takes place yielding the oxo-bridged mixed valent $Fe^{II}Fe^{III}$ complex. Were the dioxygen to bind to the metal one would expect some exchange in the oxo bridge to result as was observed in reactions of **1**-H with dioxygen that were carried out in methanol. This conclusion is further supported by the use of MMNO in which an oxo, rather than a peroxo, intermediate would be formed that would be more likely to remain coordinated in the product. Outer-sphere reaction between iron(II) complexes and dioxygen are well documented[54] and could occur in non-heme enzyme active sites where high valent iron intermediates are not required. The green intermediates observed during reactions in $CHCl_3$ solutions in earlier studies[16c,33] are likely to be **2**-H. Quantitative analyses of EPR spectra have been used to verify the presence

(52) Murray, K. S. *Coord. Chem. Rev.* **1974**, *12*, 1−35. (b) Kurtz, D. M., Jr. *Chem. Rev.* **1990**, *90*, 585−606.

(53) Ding, X.-Q.; Bominaar, E. L.; Bill, E.; Winkler, H.; Trautwein, A. X.; Drüeke, S.; Chaudhuri, P.; Wieghardt, K. *J. Chem. Phys.* **1990**, *92*, 178−186.

(54) Dickerson, L. D.; Sauer-Masarwa, A.; Herron, N.; Fendrick, C. M.; Busch, D. H. *J. Am. Chem. Soc.* **1993**, *115*, 3623−3626. (b) Sauer-Masarwa, A.; Dickerson, L. D.; Herron, N.; Busch, D. H. *Coord. Chem. Rev.* **1993**, *128*, 117−137. (c) Busch, D. H.; Alcock, N. W. *Chem. Rev.* **1994**, *94*, 585−623.

of **2** and in conjunction with the magnetization data indicate that the irons are strongly antiferromagnetically coupled. The Mössbauer data indicate that **2** is a class II mixed valence complex with distinguishable irons, although the ligands on the irons are indistinguishable on the time scale of the NMR experiment.

Acknowledgment. This research was supported by the National Institutes of Health (GM 46506). The X-ray facilities at Emory were obtained through a grant from the NIH (S10 RR07323) and we thank Dr. Victor Young, University of Minnesota, for data collection on compound **2**-Ph-OTf. We thank Shuxian Chen and Boi Hanh Huynh for Mössbauer data and for help with the EPR spectra and Robert Orosz and Edmund P. Day for magnetization data and analysis, and Dr. F. Strobel for ESI-MS data.

Supporting Information Available: Plots displaying the full atom labeling scheme for complexes **1**-Ph-OTf, **1**-Ph-BPh_4, **2**−Ph-OTf, **2**-Ph-BPh_4, **3**-Ph-OTf, and **3**-Ph-BPh_4 (Figures S−-S6) and end-on views of all Me_3tacn ligands showing λ or δ configurations of NCH_2CH_2N groups (Figures S7a−f); electronic absorption spectra of **1**-Me and **1**-F reacting with O_2 in CH_3CN (Figure S8, S9), and ESI-mass spectra of 20 μM solutions of **1**-Me-^{18}OH, **1**-Me-^{18}OH + $^{16}O_2$, **2**-Me-^{18}O, and **2**-Me-^{16}O (Figure S10); crystallographic tables for six structures (PDF). The six X-ray crystallographic files, in CIF format, are also available on the Internet. This material is available free of charge via the Internet at http://pubs.acs.org.

JA991885L